Stochastic Optical Solitons in Magneto-Optic Waveguides: Exact Solutions of a Perturbed Resonant Coupled NLSE with Dual-Power Law Nonlinearity and Multiplicative Noise

Abeer M. M. Hasek[1,3], Nouria Arar[2], Khaled A. E. Alurrfi*[3], and Abdulmalik A. Altwaty[4]

[1]Applied Mathematics and Modeling Laboratory, Department of Mathematics, University Constantine 1, Constantine, Algeria , abeer.haseek@doc.umc.edu.dz
[2]Mathematics and Decision Sciences Laboratory (LAMASD), University Constantine 1, Constantine, Algeria , arar.nouria@umc.edu.dz
[3]Department of Mathematics, Faculty of Science, Elmergib University, Khoms, Libya , alurrfi@yahoo.com
[4]Department of Mathematics, Faculty of Science, University of Benghazi, Almarj, Libya , abdulmalik.altwaty@uob.edu.ly

Abstract

This work investigates the propagation of optical solitons in magneto-optic waveguides under the guidance of a perturbed resonant coupled nonlinear Schrödinger equation (NLSE) with spatio-temporal dispersion (STD), inter-modal dispersion (IMD), dual-power law nonlinearity, and multiplicative white noise in the Itô sense. With the aid of two advanced analytical techniques, the generalized Liénard equation and the improved direct algebraic method, we derive an exhaustive set of soliton solutions, namely dark, bright, singular, and straddled solitons, and Jacobi- and Weierstrass-elliptic function solutions. These solutions are rigorously verified by numerical simulations, which determine soliton stability and robustness at varied noise levels. Our findings reveal new evidence that multiplicative noise, instead of being destabilizing, is able to modulate soliton dynamics at the cost of structural integrity, and hence present valuable insights into application potential in noisy optical media. This work fills a significant gap in nonlinear optics by solving stochastic effects in magneto-optic waveguides, paving the way for sophisticated soliton-based communication systems and photonic devices.

Keywords: Optical solitons; Magneto-optic waveguides; Stochastic NLSE; Dual-power law nonlinearity; Lienard equation; Soliton stability.
OCIS: 060.2310; 060.4510; 060.5530; 190.3270; 190.4370.

1. Introduction

The significance of nonlinear systems of partial differential equations (PDEs) in explaining various phenomena in the physical sciences, such as nonlinear optical fibers, nonlinear waveguides, quantum optics, fluid dynamics, nuclear physics, and plasma physics, is widely recognized. In recent years, numerous researchers have focused on the exploration of explicit soliton solutions for nonlinear PDEs, employing a variety of techniques [1-31]. The nonlinear Schrödinger equation (NLSE), renowned for its solitary solutions, has emerged as a prominent framework for describing wave behavior in numerous nonlinear applications. Considered a fundamental model in modern nonlinear science, the NLSE primarily governs the propagation of optical solitons. Furthermore, there has been considerable interest in investigating generalized NLSEs with constant coefficients, which are regarded as ideal models and have been extensively studied in references [1-29]. The modeling of nonlinear dynamics in optical solitons and Madelung fluids commonly involves the use of a generic resonant NLSE. It is essential, particularly when studying chiral solitons in the quantum Hall effect, to consider a specific resonant term [20-28]. Moreover, it is important to recognize that precisely defining the equation governing the propagation of optical solitons in nonlinear media requires considering the additional effects of STD and IMD [26-28].

This article presents a study on a coupled system of perturbed resonant NLSE in magneto-optic waveguides. The system incorporates STD, IMD, nonlinear dual-power law, and multiplicative noise in the Itô sense. The details of the paper are presented in the following sections.

2. The mathematical model

The single form of perturbed resonant NLSE in polarization preserving fibers under the influence of nonlinear dual-power law, STD, IMD and multiplicative white noise in the Itô sense is written as [26]:

$$i\phi_t + a\phi_{xx} + b\phi_{xt} + \left(c\left|\phi\right|^{2n} + d\left|\phi\right|^{4n}\right)\phi + \gamma\left(\frac{|\phi|_{xx}}{|\phi|}\right)\phi + \sigma\left(\phi - ib\phi_x\right)\frac{dW(t)}{dt} = i\delta\phi_x, \qquad (1)$$

where a, b, c, d, γ, δ, and σ are constants with $i = \sqrt{-1}$, and $\phi(x,t)$ is a complex-valued function that represents the wave profile. The coefficients of chromatic dispersion (CD) and STD, respectively, are represented by the constants a and b, whereas the first term in equation (1) represents the linear temporal development. The coefficient of resonant nonlinearity is the constant γ, whereas the coefficients of self-phase modulation (SPM) are c and d. The IMD's coefficient is the constant δ. Lastly, $dW(t)/dt$ is the white noise, where σ is the noise intensity coefficient and $W(t)$ is the normal Wiener process.

In birefringent fibers, equation (1) splits into two components, for the first time, as:

$$\begin{gathered} iu_t + a_1 u_{xx} + b_1 u_{xt} + \left(c_1 |u|^{2n} + d_1 |v|^{2n}\right) u + \left(e_1 |u|^{4n} + f_1 |u|^{2n} |v|^{2n} + g_1 |v|^{4n}\right) u \\ + h_1 \left(\frac{|u|_{xx}}{|u|}\right) u + \sigma \left(u - i b_1 u_x\right) \frac{dW(t)}{dt} = Q_1 v + i \left[\lambda_1 u_x + \mu_1 \left(|u|^{2n} u\right)_x \right. \\ \left. + \theta_1 \left(|u|^{2n}\right)_x u + r_1 |u|^{2n} u_x\right], \end{gathered} \tag{2}$$

and

$$\begin{gathered} iv_t + a_2 v_{xx} + b_2 v_{xt} + \left(c_2 |v|^{2n} + d_2 |u|^{2n}\right) v + \left(e_2 |v|^{4n} + f_2 |v|^{2n} |u|^{2n} + g_2 |u|^{4n}\right) v \\ + h_2 \left(\frac{|v|_{xx}}{|v|}\right) v + \sigma \left(v - i b_2 v_x\right) \frac{dW(t)}{dt} = Q_2 u + i \left[\lambda_2 v_x + \mu_2 \left(|v|^{2n} v\right)_x \right. \\ \left. + \theta_2 \left(|v|^{2n}\right)_x v + r_2 |v|^{2n} v_x\right], \end{gathered} \tag{3}$$

where $u(x,t)$ and $v(x,t)$ are functions with complex-valued that depict the wave shapes. The constants a_j and b_j for $(j = 1,2)$ represent the coefficients of CD and STD along the x and y directions, respectively. The constants c_j and d_j, $(j = 1,2)$ are the coefficients of SPM and cross-phase modulation (XPM) respectively. The constants e_j, f_j and g_j, $(j = 1,2)$ are the coefficients of nonlinear dispersion terms. The constants h_j, $(j = 1,2)$ are the coefficients of resonant nonlinearity. The constants σ_j, $(j = 1,2)$ are the coefficients of noises strength and $W(t)$ is the standard Wiener processes, such that $dW(t)/dt$ is the white noises. Finally, the constants λ_j, μ_j, θ_j and υ_j, $(j = 1,2)$ are the coefficients of the IMD, self-steepening (SS) terms and nonlinear dispersions terms respectively.
This article aims to deduce the optical solitons solutions for equations (2) and (3) directly based on the generalized nonlinear Liénard equation and the improved direct algebraic approach.

3. Converting and Mathematical Analysis

To transform equations (2) and (3) into ordinary differential equations (ODEs), we consider the wave transformations to be of the following forms:

$$u(x,t) = \phi_1(\xi) \exp\left[i(F(x,t) + \sigma W(t) - \sigma^2 t)\right], \tag{4}$$

$$v(x,t) = \phi_2(\xi) \exp\left[i\left(F(x,t) + \sigma W(t) - \sigma^2 t\right)\right], \tag{5}$$

$$\xi = x - \rho t, \;\; F(x,t) = -\kappa x + \omega t, \tag{6}$$

where κ, ω and ρ are nonzero real-valued constants such κ represents the frequency of the soliton, ω denotes the wave number, and ρ indicates the soliton's velocity. The functions $\phi_j(\xi)$ for $j = 1,2$ are real-valued functions that denote the amplitude parts of the solitons and the phase elements

of the solitons, respectively. By inserting (4)-(6) into equations (2) and (3), we obtain the real components:

$$\begin{aligned}&\left(-\rho b_1+a_1+h_1\right)\phi_1''+\left[c_1-\kappa\left(r_1+\mu_1\right)\right]\phi_1^{1+2n}+f_1\phi_2^{2n}\phi_1^{1+2n}+d_1\phi_2^{2n}\phi_1\\&+e_1\phi_1^{1+4n}+g_1\phi_2^{4n}\phi_1+\left[-\kappa^2a_1+\kappa\left(\left(-\sigma^2+\omega\right)b_1-\lambda_1\right)+\sigma^2-\omega\right]\phi_1-\phi_2Q_1=0,\end{aligned}\tag{7}$$

and

$$\begin{aligned}&\left(-\rho b_2+a_2+h_2\right)\phi_2''+\left[c_2-\kappa\left(r_2+\mu_2\right)\right]\phi_2^{1+2n}+f_2\phi_1^{2n}\phi_2^{1+2n}+d_2\phi_1^{2n}\phi_2\\&+e_2\phi_2^{1+4n}+g_2\phi_1^{4n}\phi_2+\left[-\kappa^2a_2+\left(\kappa\left(-\sigma^2+\omega\right)b_2-\lambda_2\right)+\sigma^2-\omega\right]\phi_2-\phi_1Q_2=0,\end{aligned}\tag{8}$$

while the imaginary parts are:

$$\left[\left(2n+1\right)\mu_1+2n\theta_1+r_1\right]\phi_1'\phi_1^{2n}+\left[\left(-\rho b_1+2a_1\right)\kappa+\left(\sigma^2-\omega\right)b_1+\lambda_1+\rho\right]\phi_1'=0,\tag{9}$$

and

$$\left[\left(2n+1\right)\mu_2+2n\theta_2+r_2\right]\phi_2'\phi_2^{2n}+\left[\left(-\rho b_2+2a_2\right)\kappa+\left(\sigma^2-\omega\right)b_2+\rho+\lambda_2\right]\phi_2'=0.\tag{10}$$

The principle of linear independence is utilized on (9) and (10) to derive the wave number ρ :

$$\rho=\frac{\left(\sigma^2-\omega\right)b_j+2a_j\kappa+\lambda_j}{\kappa b_j-1},\tag{11}$$

and

$$\left(2n+1\right)\mu_j+2n\theta_j+r_j=0,$$

provided $\kappa b_j\neq 1$ where $j=1,2$.
Now, let us set

$$\phi_2=\vartheta\phi_1,\tag{12}$$

where ϑ is a nonzero constant with $\vartheta\neq 1$. Equations (7) and (8) can be simplified as follows:

$$\begin{aligned}&\left(-\rho b_1+a_1+h_1\right)\phi_1''+\left(\vartheta^{2n}f_1+\vartheta^{4n}g_1+e_1\right)\phi_1^{1+4n}+\left[\vartheta^{2n}d_1-\left(r_1+\mu_1\right)\kappa+c_1\right]\phi_1^{1+2n}\\&-\left[\kappa^2a_1+\left(\left(\sigma^2-\omega\right)b_1+\lambda_1\right)\kappa+\vartheta Q_1-\sigma^2+\omega\right]\phi_1=0,\end{aligned}\tag{13}$$

and

$$\begin{aligned}&\vartheta\left(-\rho b_2+a_2+h_2\right)\phi_1''+\left(\vartheta^{1+2n}f_2+\vartheta^{1+4n}e_2+\vartheta g_2\right)\phi_1^{1+4n}+\left[\left(\left(-r_2-\mu_2\right)\kappa+c_2\right)\vartheta^{1+2n}+\vartheta d_2\right]\phi_1^{1+2n}\\&-\left[\vartheta\left(\kappa^2a_2+\left(\left(\sigma^2-\omega\right)b_2+\lambda_2\right)\kappa+\omega-\sigma^2\right)+Q_2\right]\phi_1=0.\end{aligned}\tag{14}$$

equations (14) and (15) hold equivalent status when the constraint conditions are met:

$$\begin{cases} -\rho\, b_1 + a_1 + h_1 = \vartheta\left(-\rho b_2 + a_2 + h_2\right), \\ \vartheta^{2n} f_1 + \vartheta^{4n} g_1 + e_1 = \vartheta\left(\vartheta^{2n} f_2 + \vartheta^{4n} e_2 + g_2\right), \\ \vartheta^{2n} d_1 - \left(r_1 + \mu_1\right)\kappa + c_1 = \vartheta\left[\left(\left(-r_2 - \mu_2\right)\kappa + c_2\right)\vartheta^{2n} + d_2\right], \\ \kappa^2 a_1 + \left(\left(\sigma^2 - \omega\right) b_1 + \lambda_1\right)\kappa + \vartheta Q_1 - \sigma^2 + \omega \\ = \vartheta\left[\kappa^2 a_2 + \left(1 + \left(\sigma^2 - \omega\right) b_2 + \lambda_2\right)\kappa + \omega - \sigma^2\right] + Q_2. \end{cases} \tag{15}$$

From (15), the soliton velocity is yielded as:

$$\omega = \frac{Q+\sigma^2-\kappa\left(\lambda_1+\sigma^2 b_1\right)-\vartheta Q_1+\vartheta\left[-\sigma^2+\kappa\left(\lambda_2+\sigma^2 b_2\right)+\kappa^2 a_2\right]-\kappa^2 a_1}{-\kappa b_1+\vartheta(\kappa b_2-1)+1}, \tag{16}$$

provided $-\kappa b_1 + \vartheta\left(\kappa b_2 - 1\right) + 1 \neq 0$.
Equation (13), can be rewritten as:

$$\phi_1'' + l_1\phi_1 + l_2\phi_1^{1+2n} + l_3\phi_1^{1+4n} = 0, \tag{17}$$

where

$$\begin{cases} l_1 = \frac{-\left[\kappa^2 a_1+\left(\left(\sigma^2-\omega\right)b_1+\lambda_1\right)\kappa+\vartheta Q_1-\sigma^2+\omega\right]}{-\rho b_1+a_1+h_1}, \\ l_2 = \frac{\vartheta^{2n} d_1-(r_1+\mu_1)\kappa+c_1}{-\rho b_1+a_1+h_1}, \\ l_3 = \frac{\vartheta^{2n} f_1+\vartheta^{4n} g_1+e_1}{-\rho b_1+a_1+h_1}, \end{cases} \tag{18}$$

provided $-\rho b_1 + a_1 + h_1 \neq 0$.
In the following sections, we will discover the optical solitons of equations (1) and (2) directly with the aid of the generalized Lièнard equation, in addition to utilizing the well-known improved direct algebraic approach.

4. Exploring optical solitons using the generalized Liénard equation

It is well-known that the generalized Liénard equation with nonlinear terms of any order has the form [30, 31]:

$$u''(\xi) + l u(\xi) + m u^{p+1}(\xi) + n u^{2p+1}(\xi) = 0, \tag{19}$$

where $l,\ m,\ n$ are constant coefficients and $p = 1, 2, 3, \ldots$.
If we substitute $p = 2n,\ l = l_1,\ m = l_2,\ n = l_3$ into equation (17), we obtain equation (19) again. By utilizing the exact solutions of equation (19) listed in [30, 31], we can derive the optical solitons

of equations (2) and (3), where l_1, l_2, and l_3 are determined by (18) as follows:

Case 1. When $l_1 < 0$, we get the following straddled soliton solutions

$$u(x,t) = \left[\frac{-l_1 l_2 \operatorname{sech}^2\left(\pm n\sqrt{-l_1}\xi\right)}{\frac{l_2^2}{n+1} - \frac{l_3 l_1 (n+1)}{2n+1}\left(1-\tanh\left(\pm n\sqrt{-l_1}\xi\right)\right)^2}\right]^{\frac{1}{2n}} \mathrm{e}^{i\left[-\kappa x+\left(\omega-\sigma^2\right)t+\sigma W(t)\right]}, \tag{20}$$

$$v(x,t) = \vartheta u(x,t). \tag{21}$$

Case 2. When $l_1 < 0$, $l_3 < 0$, we get the following straddled soliton solutions

$$u(x,t) = \left[\frac{-l_1 \operatorname{csch}^2\left(n\sqrt{-l_1}\xi\right)}{-\frac{l_2}{n+1} + 2\sqrt{\frac{l_3 l_1}{2n+1}}\coth\left(n\sqrt{-l_1}\xi\right)}\right]^{\frac{1}{2n}} \mathrm{e}^{i\left[-\kappa x+\left(\omega-\sigma^2\right)t+\sigma W(t)\right]}, \tag{22}$$

$$v(x,t) = \vartheta u(x,t), \tag{23}$$

$$u(x,t) = \left[\frac{-4l_1\left(\cosh\left(2n\sqrt{-l_1}\xi\right)+\sinh\left(2n\sqrt{-l_1}\xi\right)\right)}{\frac{4l_3 l_1}{2n+1} - \left(-\frac{l_2}{n+1}+\cosh\left(2n\sqrt{-l_1}\xi\right)+\sinh\left(2n\sqrt{-l_1}\xi\right)\right)^2}\right]^{\frac{1}{2n}} \mathrm{e}^{i\left[-\kappa x+\left(\omega-\sigma^2\right)t+\sigma W(t)\right]}, \tag{24}$$

$$v(x,t) = \vartheta u(x,t), \tag{25}$$

$$u(x,t) = \left[8l_1^2 \operatorname{sech}\left(2n\sqrt{-l_1}\xi\right) \Big/ \left(\frac{l_2^2}{(n+1)^2} - 4l_1\left(-l_1 + \frac{l_3}{2n+1}\right)\right.\right.$$

$$\left.\left.\left(-\frac{4l_2 l_1}{(n+1)} \operatorname{sech}\left(2n\sqrt{-l_1}\xi\right) - 4l_1\left(l_1 + \frac{l_3}{2n+1}\right)\tanh\left(2n\sqrt{-l_1}\xi\right)\right)\right]^{\frac{1}{2n}} \tag{26}$$

$$\times\, \mathrm{e}^{i\left[-\kappa x+\left(\omega-\sigma^2\right)t+\sigma W(t)\right]},$$

$$v(x,t) = \vartheta u(x,t), \tag{27}$$

$$u(x,t) = \left[\frac{-l_1 \operatorname{csch}\left(n\sqrt{-l_1}\xi\right)}{-\frac{l_2}{n+1}\sinh\left(n\sqrt{-l_1}\xi\right) + 2\sqrt{\frac{l_3 l_1}{2n+1}}\cosh\left(n\sqrt{-l_1}\xi\right)}\right]^{\frac{1}{2n}} \mathrm{e}^{i\left[-\kappa x+\left(\omega-\sigma^2\right)t+\sigma W(t)\right]}, \tag{28}$$

$$v(x,t) = \vartheta u(x,t), \tag{29}$$

$$u(x,t) = \left[\frac{-l_1 \operatorname{sech}\left(n\sqrt{-l_1}\xi\right)}{2\sqrt{\frac{l_3 l_1}{2n+1}}\sinh\left(n\sqrt{-l_1}\xi\right) + \frac{l_2}{n+1}\cosh\left(n\sqrt{-l_1}\xi\right)}\right]^{\frac{1}{2n}} \mathrm{e}^{i\left[-\kappa x+\left(\omega-\sigma^2\right)t+\sigma W(t)\right]}, \tag{30}$$

$$v(x,t) = \vartheta u(x,t). \tag{31}$$

Case 3. When $l_1 < 0$ and $\frac{l_2^2}{4(n+1)^2} - \frac{l_3 l_1}{2n+1} > 0$, we get the following soliton solutions:

$$u(x,t) = \left[\frac{2l_1(n+1)}{-l_2 \pm 2(n+1)\sqrt{\frac{l_2^2}{4(n+1)^2} - \frac{l_3 l_1}{2n+1}}\cosh\left(2n\sqrt{-l_1}\xi\right)}\right]^{\frac{1}{2n}} \mathrm{e}^{i\left[-\kappa x+\left(\omega-\sigma^2\right)t+\sigma W(t)\right]}, \tag{32}$$

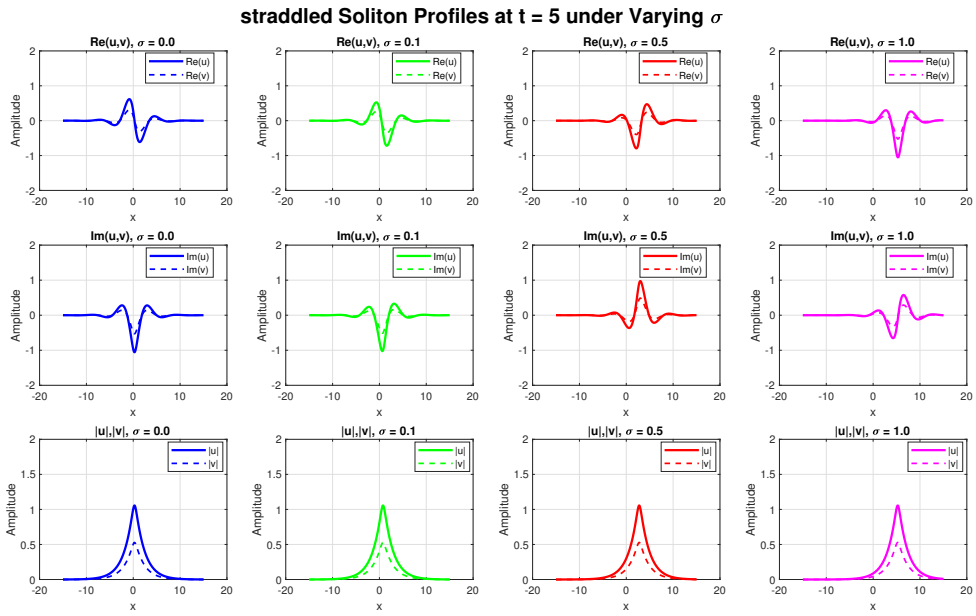

(a) Real and Imaginary Parts with Magnitude Profiles.

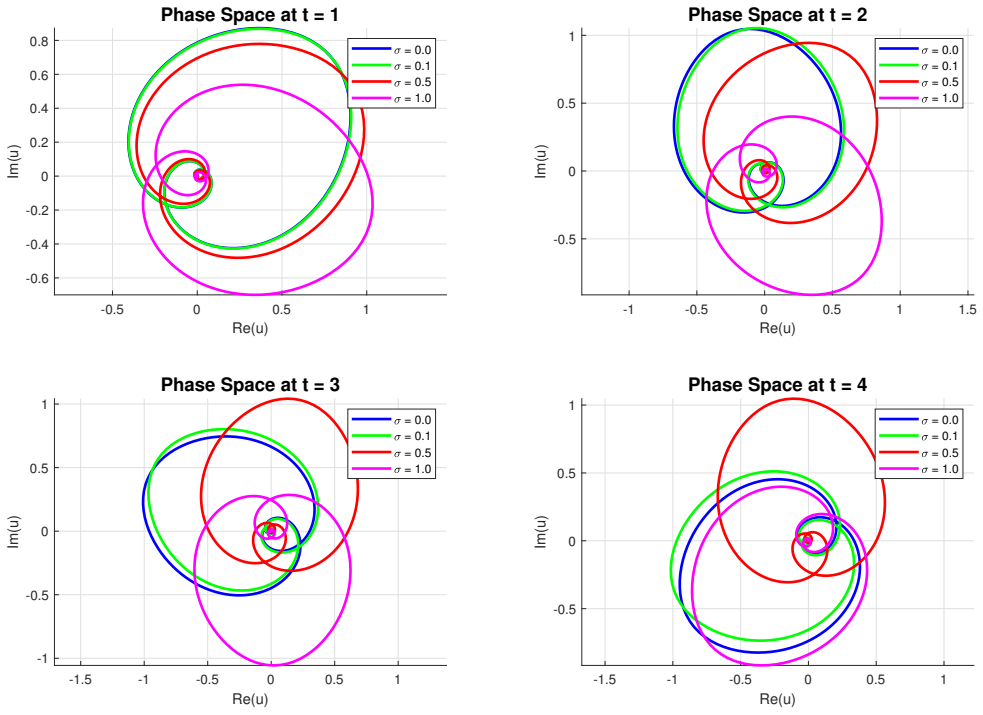

(b) Phase Space Profiles.

Figure 1: straddled soliton solution Eqs.(20) and (21) at $t = 5$, $W(t) = \sqrt{t}$, $n = 2$, $\omega = \kappa = l_2 = l_3 = 1, l_1 = -1$, $\rho = 0.5$, and varying noise strength σ. (a) shows the real and imaginary components of the coupled fields with heir magnitude profiles, while (b) presents Phase Space profiles.

$$v(x,t) = \vartheta u(x,t). \tag{33}$$

Case 4. When $l_1 < 0$ and $\frac{l_2^2}{4(n+1)^2} - \frac{l_3 l_1}{2n+1} < 0$, we get the following singular soliton solutions:

$$u(x,t) = \left[\frac{l_1 \operatorname{csch}\left(2n\sqrt{-l_1}\xi\right)}{\pm\sqrt{\frac{l_3 l_1}{2n+1} - \frac{l_2^2}{4(n+1)^2}} - \frac{l_2}{2(n+1)}\operatorname{csch}\left(2n\sqrt{-l_1}\xi\right)}\right]^{\frac{1}{2n}} \mathrm{e}^{i\left[-\kappa x + \left(\omega-\sigma^2\right)t + \sigma W(t)\right]}, \tag{34}$$

$$v(x,t) = \vartheta u(x,t). \tag{35}$$

Case 5. When $l_1 < 0$ and $\frac{l_2^2}{4(n+1)^2} - \frac{l_3 l_1}{2n+1} = 0$, we get the dark-soliton solutions

$$u(x,t) = \left[-\frac{l_1(n+1)}{l_2}\left(1 \pm \tanh\left(n\sqrt{-l_1}\xi\right)\right)\right]^{\frac{1}{2n}} \mathrm{e}^{i\left[-\kappa x + \left(\omega-\sigma^2\right)t + \sigma W(t)\right]}, \tag{36}$$

$$v(x,t) = \vartheta u(x,t), \tag{37}$$

and the singular soliton solutions

$$u(x,t) = \left[-\frac{l_1(n+1)}{l_2}\left(1 \pm \coth\left(n\sqrt{-l_1}\xi\right)\right)\right]^{\frac{1}{2n}} \mathrm{e}^{i\left[-\kappa x + \left(\omega-\sigma^2\right)t + \sigma W(t)\right]}, \tag{38}$$

$$v(x,t) = \vartheta u(x,t). \tag{39}$$

Case 6. When $l_2 = 0$, we get the bright-soliton solutions

$$u(x,t) = \left[\pm\sqrt{-\frac{l_1(2n+1)}{l_3}}\operatorname{sech}\left(2n\sqrt{-l_1}\xi\right)\right]^{\frac{1}{2n}} \mathrm{e}^{i\left[-\kappa x + \left(\omega-\sigma^2\right)t + \sigma W(t)\right]}, \tag{40}$$

$$v(x,t) = \vartheta u(x,t), \tag{41}$$

provided $l_1 < 0,\ l_3 > 0$, and singular soliton solutions

$$u(x,t) = \left[\pm\sqrt{\frac{l_1(2n+1)}{l_3}}\operatorname{csch}\left(2n\sqrt{-l_1}\xi\right)\right]^{\frac{1}{2n}} \mathrm{e}^{i\left[-\kappa x + \left(\omega-\sigma^2\right)t + \sigma W(t)\right]}, \tag{42}$$

$$v(x,t) = \vartheta u(x,t), \tag{43}$$

provided $l_1 < 0,\ l_3 < 0$.

Case 7. When $l_3 = 0$ and $l_1 < 0$, we get the bright-soliton solutions

$$u(x,t) = \left[-\frac{l_1(n+1)}{l_2}\operatorname{sech}^2\left(n\sqrt{-l_1}\xi\right)\right]^{\frac{1}{2n}} \mathrm{e}^{i\left[-\kappa x + \left(\omega-\sigma^2\right)t + \sigma W(t)\right]}, \tag{44}$$

$$v(x,t) = \vartheta u(x,t), \tag{45}$$

provided $l_2 > 0$, and singular soliton solutions

$$u(x,t) = \left[\frac{l_1(n+1)}{l_2}\operatorname{csch}^2\left(n\sqrt{-l_1}\xi\right)\right]^{\frac{1}{2n}} \mathrm{e}^{i\left[-\kappa x + \left(\omega-\sigma^2\right)t + \sigma W(t)\right]}, \tag{46}$$

$$v(x,t) = \vartheta u(x,t), \tag{47}$$

provided $l_2 < 0$.

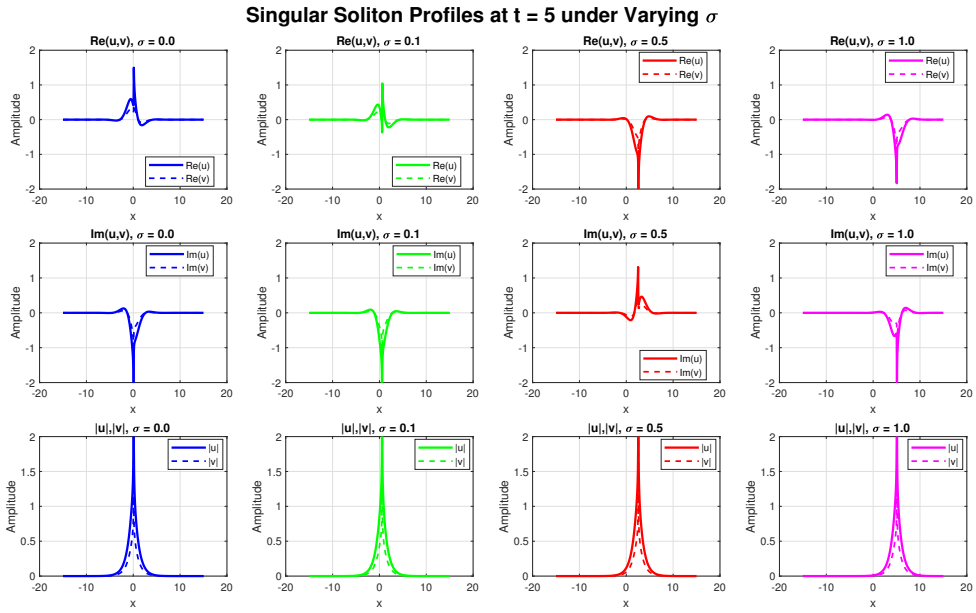

(a) Real and Imaginary Parts with Magnitude Profiles.

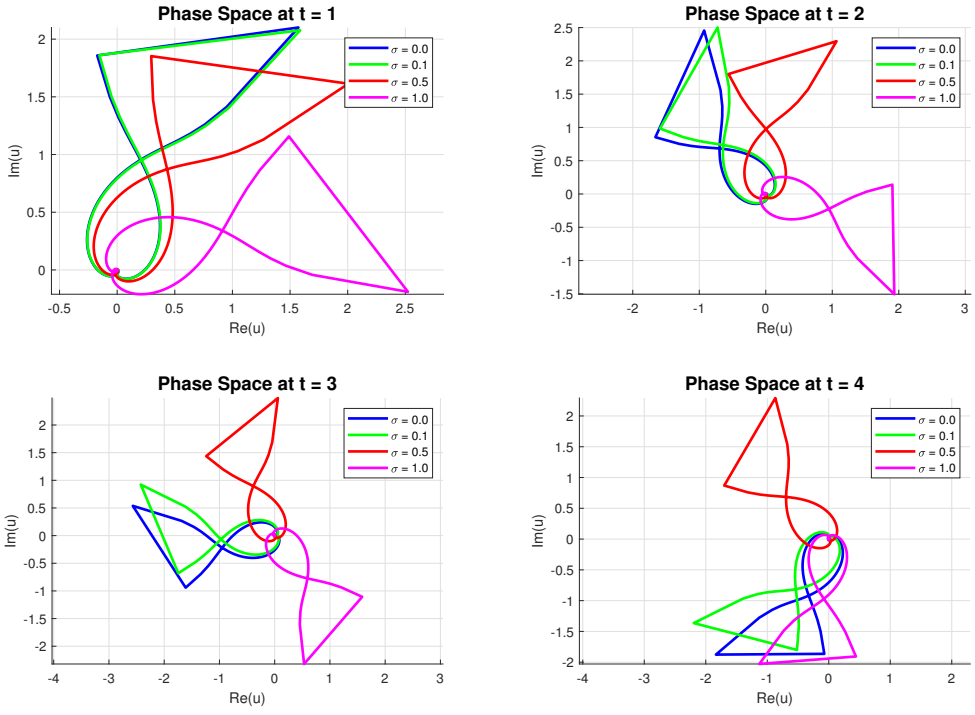

(b) Phase Space Profiles.

Figure 2: singular soliton solution Eqs.(20) and (21) at $t = 5$, $W(t) = \sqrt{t}$, $n = 2$, $\omega = \kappa = l_2 = l_3 = 1$,$l_1 = -1$, $\rho = 0.5$, and varying noise strength σ. (a) shows the real and imaginary components of the coupled fields with heir magnitude profiles, while (b) presents Phase Space profiles.

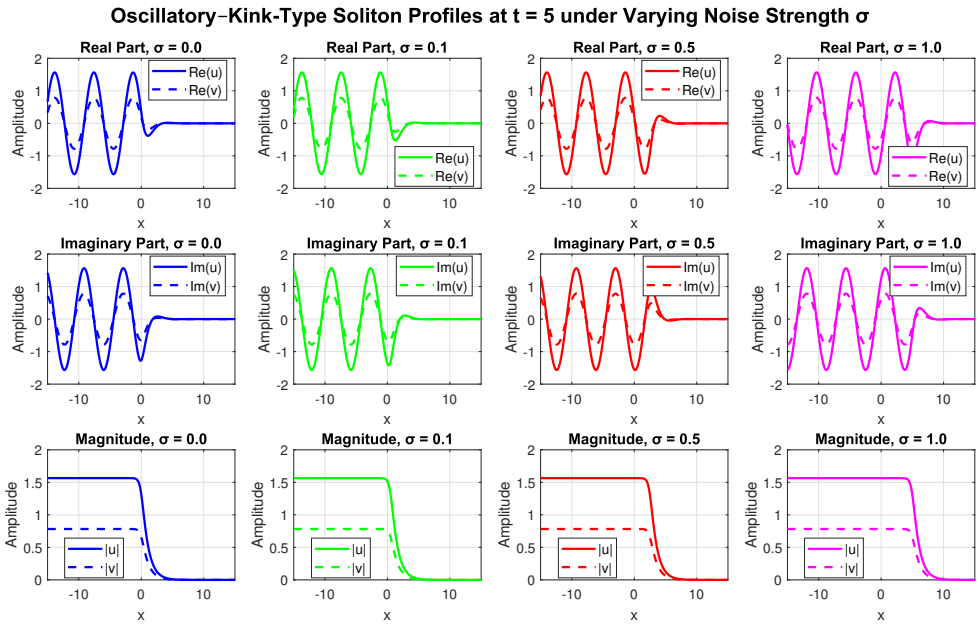

(a) Real and Imaginary Parts with Magnitude Profiles.

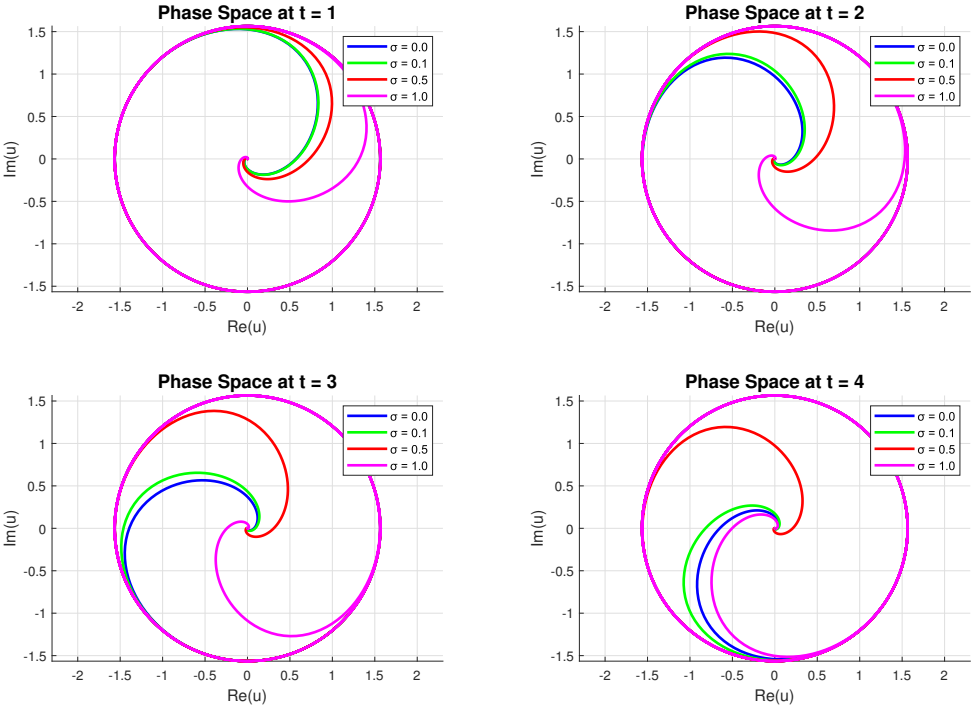

(b) Phase Space Profiles.

Figure 3: Oscillatory–Kink-Type Soliton Structures at $t = 5$, $W(t) = \sqrt{t}$, $n = 2$, $\omega = \kappa = l_2 = 1$,$l_1 = -1$, $\rho = 0.5$, and varying noise strength σ. (a) shows the real and imaginary components of the coupled fields with heir magnitude profiles, while (b) presents Phase Space profiles.

5. An improved direct algebraic approach

Let us now, solve equation (17) under the constraint conditions (18) as follows:
First, balancing $\phi_1''(\xi)$ and $\phi_1^{4n+1}(\xi)$ in equation (17) gives $N = \frac{1}{2n}$. Therefore, the new wave transformation:

$$\phi_1 = [H(\xi)]^{\frac{1}{2n}}, \tag{48}$$

where the new function $H(\xi) > 0$, changes equation (17) to the following new nonlinear ODE:

$$2nHH'' + (1-2n)H'^2 + 4n^2H^2(l_3H^2 + l_2H + l_1) = 0. \tag{49}$$

The improved direct algebraic approach introduced by Arnous et al. [29] supposes that equation (49) has the following formal solution:

$$H(\xi) = \sum_{k=0}^{N} A_k \psi^k(\xi), \tag{50}$$

where $A_0,\ A_k\ (k = 1, 2, ..., N)$ are constants such that $A_N \neq 0$. While the function $\psi(\xi)$ holds the nonlinear ODE:

$$\psi'^2(\xi) = \sum_{r=0}^{4} \tau_r \psi^r(\xi), \tag{51}$$

where $\tau_r\ (r = 0,\ 1,\ 2,\ 3,\ 4)$ are constants such that $\tau_4 \neq 0$. It is well-known [29] that equation (49) has many types of exact solutions.
Now, balancing the terms HH'' and H^4 in equation (49), outputs the balance number $N = 1$. Consequently, the formula solution (50) takes the following form:

$$H(\xi) = A_0 + A_1\psi(\xi), \tag{52}$$

where $A_1 \neq 0$.
By substituting (52) along with (51) into equation (49) and using Maple, there are many families of results that will be discussed as follows:
Family-1. When $\tau_0 = \tau_1 = \tau_3 = 0$, we have the following results:
Result 1.

$$n = n,\ A_0 = 0,\ A_1 = \sqrt{-\frac{\tau_4(2n+1)}{4n^2 l_3}},\ l_1 = -\frac{\tau_2}{4n^2},\ l_2 = 0, \tag{53}$$

provided $l_3\tau_4 < 0$.
By substituting (53) with the well-known solutions of equation (51) mentioned in [29] into (52) and using (48) as well as (4), (5), two types of soliton solutions can be derived as follows:

I. If $\tau_2 > 0$ and $\tau_4 < 0$, then we have the bright-soliton solutions

$$u(x,t) = \left\{ \sqrt{\frac{\tau_2(2n+1)}{4n^2 l_3}}\, \operatorname{sech}\left(\sqrt{\tau_2}\xi\right) \right\}^{\frac{1}{2n}} \mathrm{e}^{i\left[-\kappa x + \left(\omega-\sigma^2\right)t + \sigma W(t)\right]}, \tag{54}$$

$$v(x,t) = \vartheta u(x,t), \tag{55}$$

provided $l_3 > 0$. **II.** If $\tau_2 > 0$ and $\tau_4 > 0$, then we have the singular soliton solutions

$$u(x,t) = \left\{ \sqrt{-\frac{\tau_2(1+2n)}{4n^2 l_3}}\, \operatorname{csch}\left(\sqrt{\tau_2}\xi\right) \right\}^{\frac{1}{2n}} \mathrm{e}^{i\left[-\kappa x + \left(\omega-\sigma^2\right)t + \sigma W(t)\right]}, \tag{56}$$

$$v(x,t) = \vartheta u(x,t), \tag{57}$$

provided $l_3 < 0$.

Result 2.

$$n = 1,\ A_0 = \sqrt{\frac{3\tau_2}{4l_3}},\ A_1 = \sqrt{-\frac{3\tau_4}{4l_3}},\ l_1 = \frac{5\tau_2}{4},\ l_2 = -\sqrt{\frac{16\tau_2 l_3}{3}}. \tag{58}$$

This result leads to the bright-soliton solutions

$$u(x,t) = \left\{ \sqrt{\frac{3\tau_2}{4l_3}} \left(1 + \operatorname{sech}\left(\sqrt{\tau_2}\xi\right)\right) \right\}^{\frac{1}{2n}} \mathrm{e}^{i\left[-\kappa x + \left(\omega-\sigma^2\right)t + \sigma W(t)\right]}, \tag{59}$$

$$v(x,t) = \vartheta u(x,t), \tag{60}$$

provided $\tau_2 > 0$, $\tau_4 < 0$ and $l_3 > 0$.

Family-2. When $\tau_0 = \frac{\tau_2^2}{4l_4}$, $\tau_1 = \tau_3 = 0$, $\tau_2 < 0$ and $\tau_4 > 0$, we have the following result:

$$n = n, A_0 = \sqrt{\frac{(4n+2)\tau_2}{16n^2 l_3}}, A_1 = \sqrt{-\frac{(2n+1)\tau_4}{4n^2 l_3}}, l_1 = \frac{\tau_2}{2n^2}, l_2 = -\sqrt{\frac{2\tau_2 l_3 (n+1)^2}{n^2(2n+1)}}, \tag{61}$$

provided $l_3 < 0$.

By substituting (61) with the well-known solutions of equation (51) mentioned in [29] into (52) and using (48) as well as (4), (5), we obtain the dark-soliton solutions:

$$u(x,t) = \left\{ \sqrt{\frac{(2n+1)\tau_2}{8n^2 l_3}} \left(1 + \tanh\left(\sqrt{-\frac{\tau_2}{2}}\xi\right)\right) \right\}^{\frac{1}{2n}} \mathrm{e}^{i\left[-\kappa x + \left(\omega-\sigma^2\right)t + \sigma W(t)\right]}, \tag{62}$$

$$v(x,t) = \vartheta u(x,t), \tag{63}$$

and the singular soliton solutions

$$u(x,t) = \left\{ \sqrt{\frac{(2n+1)\tau_2}{8n^2 l_3}} \left(1 + \coth\left(\sqrt{-\frac{\tau_2}{2}}\xi\right)\right) \right\}^{\frac{1}{2n}} \mathrm{e}^{i\left[-\kappa x + \left(\omega-\sigma^2\right)t + \sigma W(t)\right]}, \tag{64}$$

$$v(x,t) = \vartheta u(x,t). \tag{65}$$

Family-3. When $\tau_1 = \tau_3 = 0$, $\tau_0 = \frac{m^2\left(1-m^2\right)\tau_2^2}{\left(2m^2-1\right)^2\tau_4}$, $\tau_2 > 0$, $\tau_4 < 0$ and $0 < m < 1$, we have the

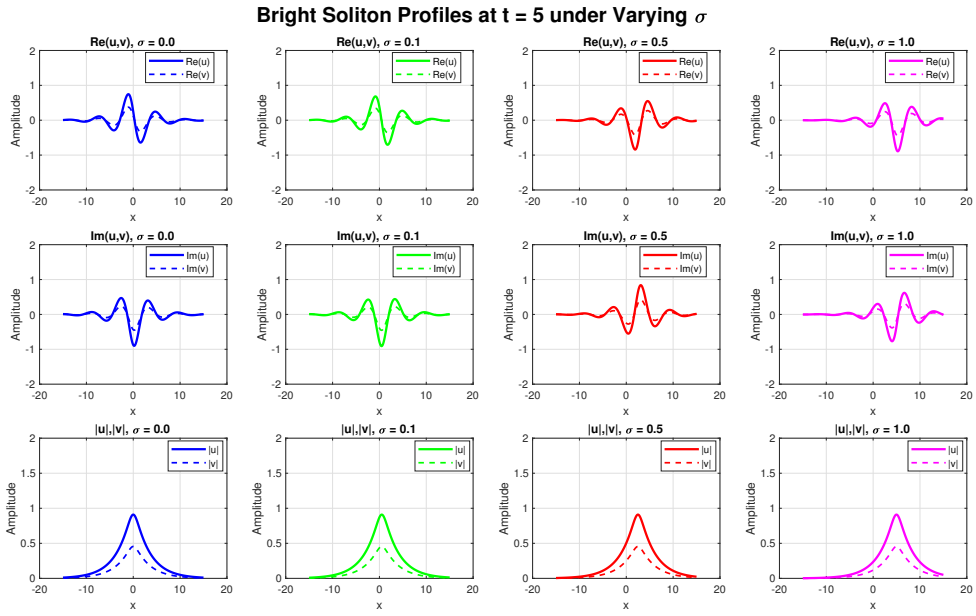

(a) Real and Imaginary Parts with Magnitude Profiles.

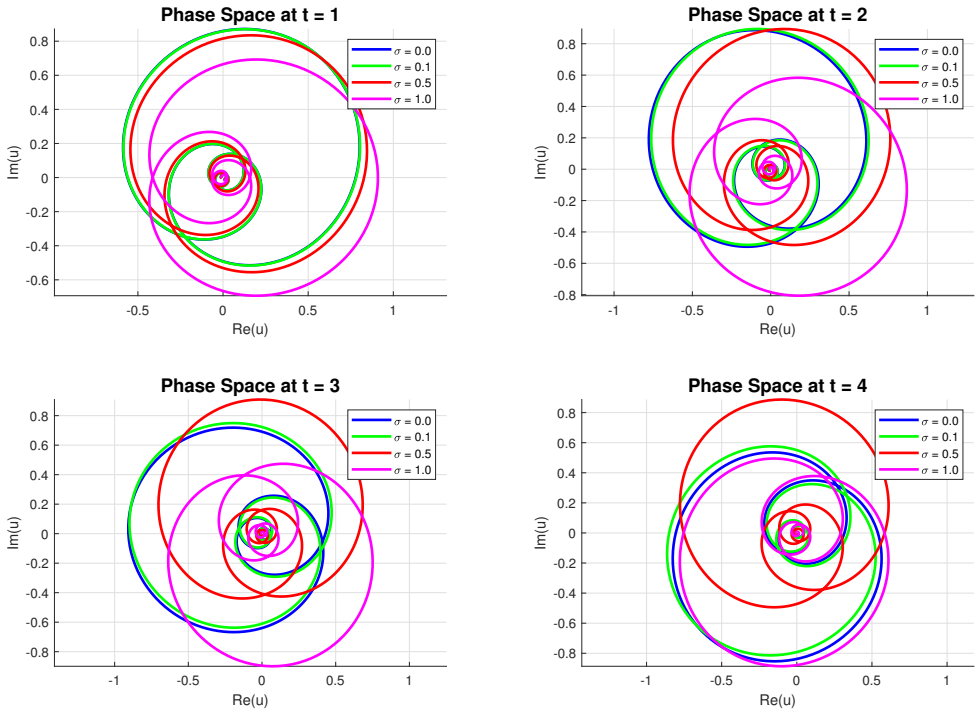

(b) Phase Space Profiles.

Figure 4: Bright Soliton solution at $t = 5$, $W(t) = \sqrt{t}$, $n = 2$, $\omega = \kappa = l_3 = 1$,$\tau_2 = 1.5$, $\tau_4 = -1$, $\rho = 0.5$, and varying noise strength σ. (a) shows the real and imaginary components of the coupled fields with heir magnitude profiles, while (b) presents Phase Space profiles.

following result:

$$m=1,\ n=n,\ A_0=0,\ A_1=\sqrt{-\frac{\tau_4\left(2n+1\right)}{4n^2l_3}},\ l_1=-\frac{\tau_2}{4n^2},\ l_2=0, \tag{66}$$

provided $l_3<0$.
By substituting (66) with the well-known solutions of equation (51) mentioned in [29] into (52) and using (48) as well as (4), (5), we have the same bright-soliton solutions (54)
Family-4. When $\tau_1=\tau_3=0,\ \tau_0=\frac{m_2^2\tau_2^2}{(m^2+1)^2\tau_4}$, $\tau_2<0$, $\tau_4>0$ and $0<m<1$, we have the following result:

$$n=1, A_0=-\frac{2m^2\tau_2}{l_2\left(m^2+1\right)}, A_1=\sqrt{-\frac{4\tau_2\tau_4m^2}{l_2^2\left(m^2+1\right)}}, l_1=\frac{\tau_2\left(5m^2-1\right)}{4m^2+4}, l_3=\frac{3l_2^2\left(m^2+1\right)}{16m^2\tau_2}. \tag{67}$$

By substituting (67) with the well-known solutions of equation (51) mentioned in [29] into (52) and using (48) as well as (4), (5), we have the Jacobi-elliptic function solutions:

$$u\left(x,t\right)=\left\{-\frac{2m^2\tau_2}{l_2(m^2+1)}\left(1+\text{JacobiSN}\left(\sqrt{-\frac{\tau_2}{m^2+1}},m\right)\right)\right\}^{\frac{1}{2n}}\mathrm{e}^{i\left[-\kappa x+\left(\omega-\sigma^2\right)t+\sigma W(t)\right]}, \tag{68}$$

$$v\left(x,t\right)=\vartheta u\left(x,t\right), \tag{69}$$

Remark In particular, if $m=1$, the Jacobi-elliptic function solutions (68) and (69) can be converted to the dark solitons

$$u\left(x,t\right)=\left\{-\frac{\tau_2}{l_2}\left(1+\tanh\left(\sqrt{-\frac{\tau_2}{2}}\right)\right)\right\}^{\frac{1}{2n}}\mathrm{e}^{i\left[-\kappa x+\left(\omega-\sigma^2\right)t+\sigma W(t)\right]}, \tag{70}$$

$$v\left(x,t\right)=\vartheta u\left(x,t\right), \tag{71}$$

Family-5. When $\tau_1=\tau_3=0,\ \tau_0>0$ and $\tau_4>0$ we have the following result:

$$n=n,\ A_0=\frac{(n+1)\sqrt{\tau_0\tau_4}}{n^2l_2},\ A_1=\frac{(n+1)\tau_0^{\frac{1}{4}}\tau_4^{\frac{3}{4}}}{l_2n^2},\ l_1=-\frac{\sqrt{\tau_0\tau_4}}{n^2}, l_3=-\frac{n^2l_2^2\left(n+\frac{1}{2}\right)}{2\left(n+1\right)^2\sqrt{\tau_0\tau_4}}, \tau_2=-2\sqrt{\tau_0\tau_4}, \tag{72}$$

By substituting (72) with the well-known solutions of equation (51) mentioned in [29] into (52) and using (48) as well as (4), (5), we have the Weierstrass-elliptic function solutions:

$$u\left(x,t\right)=\left\{\frac{\left(\tau_0\tau_4\right)^{\frac{1}{4}}(n+1)}{l_2n^2}\left(\left(\tau_0\tau_4\right)^{\frac{1}{4}}+\frac{3\wp'\left(\xi;\frac{\tau_2^2}{12}+\tau_0\tau_4,\frac{\tau_2\left(36\tau_0\tau_4-\tau_2^2\right)}{216}\right)}{6\wp\left(\xi;\frac{\tau_2^2}{12}+\tau_0\tau_4,\frac{\tau_2\left(36\tau_0\tau_4-\tau_2^2\right)}{216}\right)+\tau_2}\right)\right\}^{\frac{1}{2n}}\mathrm{e}^{i\left[-\kappa x+\left(\omega-\sigma^2\right)t+\sigma W(t)\right]}, \tag{73}$$

$$v\left(x,t\right)=\vartheta u\left(x,t\right), \tag{74}$$

and

$$u\left(x,t\right)=\left\{\frac{(n+1)\sqrt{\tau_0\tau_4}}{n^2l_2}\left(1+\frac{6(\tau_0\tau_4)^{\frac{1}{4}}\wp\left(\xi;\frac{\tau_2^2}{12}+\tau_0\tau_4,\frac{\tau_2\left(36\tau_0\tau_4-\tau_2^2\right)}{216}\right)+\tau_2}{3\wp'\left(\xi;\frac{\tau_2^2}{12}+\tau_0\tau_4,\frac{\tau_2\left(36\tau_0\tau_4-\tau_2^2\right)}{216}\right)}\right)\right\}^{\frac{1}{2n}}\mathrm{e}^{i\left[-\kappa x+\left(\omega-\sigma^2\right)t+\sigma W(t)\right]},\tag{75}$$

$$v\left(x,t\right)=\vartheta u\left(x,t\right).\tag{76}$$

Family-6. When $\tau_0=\tau_1=0$ and $\tau_2>0$, we have the following result:

$$n=n,\ A_0=0,\ A_1=\sqrt{-\tfrac{\tau_4(1+2n)}{4l_3n^2}},\ l_1=-\frac{\tau_2}{4n^2},\ l_2=\tfrac{\tau_3(n+1)}{2n}\sqrt{-\tfrac{l_3}{\tau_4(1+2n)}},\tag{77}$$

provided $l_3\tau_4<0$.
By substituting (77) with the well-known solutions of equation (51) mentioned in [29] into (52) and using (48) as well as (4), (5), many types of straddled soliton solutions can be derived as follows:

$$u\left(x,t\right)=\left\{-\sqrt{-\tfrac{\tau_4(1+2n)}{l_3n^2}}\left(\frac{\tau_2\,\mathrm{sech}^2\left(\frac{\sqrt{\tau_2}\,\xi}{2}\right)}{4\sqrt{\tau_2\tau_4}\,\tanh\left(\frac{\sqrt{\tau_2}\,\xi}{2}\right)+2\tau_3}\right)\right\}^{\frac{1}{2n}}\mathrm{e}^{i\left[-\kappa x+\left(\omega-\sigma^2\right)t+\sigma W(t)\right]},\tag{78}$$

$$v\left(x,t\right)=\vartheta u\left(x,t\right),\tag{79}$$

$$u\left(x,t\right)=\left\{\sqrt{-\tfrac{\tau_4(1+2n)}{l_3n^2}}\left(\frac{\tau_2\,\mathrm{csch}^2\left(\frac{\sqrt{\tau_2}\,\xi}{2}\right)}{4\sqrt{\tau_2\tau_4}\,\coth\left(\frac{\sqrt{\tau_2}\,\xi}{2}\right)+2\tau_3}\right)\right\}^{\frac{1}{2n}}\mathrm{e}^{i\left[-\kappa x+\left(\omega-\sigma^2\right)t+\sigma W(t)\right]},\tag{80}$$

$$v\left(x,t\right)=\vartheta u\left(x,t\right),\tag{81}$$

$$u\left(x,t\right)=\left\{\sqrt{-\tfrac{\tau_4(1+2n)}{l_3n^2}}\left(-\frac{\tau_2\tau_3\,\mathrm{sech}^2\left(\frac{\sqrt{\tau_2}\,\xi}{2}\right)}{2\tau_3^2-2\tau_2\tau_4\left(1-\tanh\left(\frac{\sqrt{\tau_2}\,\xi}{2}\right)\right)^2}\right)\right\}^{\frac{1}{2n}}\mathrm{e}^{i\left[-\kappa x+\left(\omega-\sigma^2\right)t+\sigma W(t)\right]},\tag{82}$$

$$v\left(x,t\right)=\vartheta u\left(x,t\right),\tag{83}$$

and

$$u\left(x,t\right)=\left\{\sqrt{-\tfrac{\tau_4(1+2n)}{l_3n^2}}\left(\frac{\tau_2\tau_3\,\mathrm{csch}^2\left(\frac{\sqrt{\tau_2}\,\xi}{2}\right)}{2\tau_3^2-2\tau_2\tau_4\left(1-\coth\left(\frac{\sqrt{\tau_2}\,\xi}{2}\right)\right)^2}\right)\right\}^{\frac{1}{2n}}\mathrm{e}^{i\left[-\kappa x+\left(\omega-\sigma^2\right)t+\sigma W(t)\right]},\tag{84}$$

$$v\left(x,t\right)=\vartheta u\left(x,t\right),\tag{85}$$

6. Results and Discussion

In this article we develop a detail study for the propagation of optical solitons travelling in magneto-optic waveguide system, as dictated by the perturbed resonant-coupled nonlinear Schrödinger equation (NLSE) with spatiotemporal dispersion (STD) and intermodal dispersion (IMD), dual power law nonlinearity, and self-induced multiplicative white noise in the Itô sense. Using two robust mathematical techniques the generalized Liénard equation and the improved direct algebraic method we successfully derived several types of optical soliton solutions, including dark

solitons, bright solitons, singular solitons, straddled solitons, Jacobi-elliptic function solutions, and Weierstrass-elliptic function solutions.

The results are visualized through a series of figures that demonstrate the evolution of these soliton structures under varying noise intensities. These figures provide critical insights into how multiplicative white noise affects the stability, shape, and dynamics of soliton propagation in such systems.

Straddled Soliton Solutions and Their Behavior

Figure 1 displays the straddled soliton profiles at $t = 5$ for different values of the noise strength σ. The real and imaginary parts of the soliton fields $u(x,t)$ and $v(x,t)$ are shown alongside their magnitudes. We obsorve that as σ rises from 0 to 1, we find that the soliton patterns remain intact but show a little amount of amplitude modulation and widening. This suggests that even with mild noise disruptions, the system maintains its stability.

Additionally, the phase space diagrams reveal how noise impacts the soliton's inner workings, showing increasingly complex paths as σ increases. When there's no noise ($\sigma = 0$), the soliton's path is tightly controlled, pointing to orderly motion. However, as noise levels go up, the path becomes more spread out, indicating random effects on the soliton's amplitude and phase.

These findings suggest that while multiplicative noise does introduce randomness, it doesn't completely dismantle the soliton's structure. Instead, it subtly alters its shape and phase features. This is really important for understanding how signals travel through noisy magnetic and optical environments.

Singular Soliton Dynamics Under Noise Perturbation

Figure 2 shows us what the singular soliton solutions look like under similar conditions. You can see that unlike straddled solitons, these singular ones have very sharp peaks and cusps – features that point to their unstable nature. However, it seems that noise tends to smooth out these sharp points over time.

When there's no noise ($\sigma = 0$), the solution has a clear, well-defined singularity. But as the noise level (σ) goes up, the sharpness of the peak decreases, and the wave itself spreads out a bit more.

The graphs showing magnitude support this idea, revealing a steady drop in peak intensity and an increase in how spread out the soliton is across space as noise gets stronger. Looking at the phase space portraits, we find that the dynamics of the singular soliton become less predictable when there's more noise; the paths they follow start covering larger areas of the phase plane. This suggests that noise could actually be used to control or adjust the sharpness and how localized these singular solitons are.

Bright Soliton Stability and Noise Influence

Figure 4 shows us what bright solitons look like under different levels of noise. We already know these solitons are tough and compact. And look here, even when they're faced with quite a bit

of noise, they still keep their classic bell shape. Both the real and imaginary parts stay neatly balanced and contained, which really highlights how resilient bright solitons are against noise.

It's interesting to note that as the noise goes up, the height (amplitude) of the soliton drops just a little, and it gets slightly wider. This kind of balancing act between height and width when noise is present is pretty important for real-world uses, especially where keeping the pulse's energy steady matters. The phase space diagrams we see here also tell a similar story, showing a shift from predictable to more random behavior. As the noise level parameter, σ, gets bigger, the paths (orbits) in the diagram spread out more.

So, this result really backs up the idea that bright solitons are a great choice for long-distance communication through noisy magnetic-optic waveguides. Their sturdy structure and ability to resist distortion from noise are key reasons why.

Oscillatory–Kink-Type Soliton Structures

Figure 3 shows us soliton structures that are a special mix of oscillations and kink-like shapes. These represent a unique type of solution that blends periodic waves with abrupt transitions. When noise levels go up, the oscillating pattern starts to look less regular, but the basic kink shape stays recognizable. This suggests that even though noise messes with the small-scale details of the oscillation, the overall kink behavior isn't really affected.

The graphs of the soliton's size show only a little bit of change, which confirms that the soliton keeps most of its energy even with the noise added. These results are especially important for things like optical switching and logic gates in all-optical devices, where having controlled transitions and specific wave behaviors is key.

Impact of Multiplicative Noise on Soliton Integrity

Interestingly, across all the different types of solitons studied, the multiplicative white noise consistently had a stabilizing effect instead of making things unstable. While the noise did cause small distortions and phase shifts, it never actually made any soliton structure break apart or collapse. This result is quite significant because many nonlinear systems are typically very sensitive to random disturbances.

We think this stabilizing effect might be linked to the Itô way of interpreting the noise term. This interpretation seems to work like a kind of damping mechanism, helping to smooth out the rapid oscillations inside the soliton. Moreover, adding both the STD and IMD terms appears to strengthen the delicate balance needed for solitons to exist, making the whole system much tougher against outside noise influences.

Significance of Elliptic Function Solutions

Along with the usual soliton solutions, we also found solutions involving Jacobi and Weierstrass elliptic functions. The Jacobi ones represent periodic waveforms, while the Weierstrass ones describe doubly periodic patterns. These are really useful for modeling long-lasting wave trains and signals that are almost periodic within magneto-optic materials. Finding these solutions shows

just how complex and varied the behavior described by our model can be, and it suggests exciting new paths for exploring intricate wave behaviors in structured environments.

Conclusion of Observations

The numerical simulations shown in Figures 1–4 bring together some important findings:

* All the different types of solitons studied—dark, bright, singular, and straddled—manage to keep their basic structure intact even when exposed to multiplicative white noise.
* As the noise gets stronger, we do see small decreases in amplitude, a slight spreading out, and some phase diffusion, but these effects don't fundamentally destroy the soliton's nature.
* These solitons' phase-space behavior is depicted in images that shift from an ordered to a more chaotic appearance, highlighting the system's random and unpredictable nature. Surprisingly, the noise appears to stabilize the solitons, increasing their robustness instead of making them unstable.
* The connection between the modes labeled u and v stays the same regardless of the noise level, meaning the fiber's birefringent properties are preserved.

These results are significant for designing and improving future magneto-optic devices, particularly those meant to work in noisy or constantly changing environments. They also strongly suggest that it's crucial to include random effects (stochastic effects) in the theoretical models we use to understand how nonlinear waves travel.

Comparison with Previous Studies

Our research takes a step beyond previous studies on light waves moving through magneto-optic waveguides, specifically those using a standard model (the NLSE) without any disturbances. While earlier work often focused on ideal, lab-like situations and ignored random effects, we've expanded the analysis by adding two important real-world factors: random noise that multiplies with the signal, and higher-order dispersion effects. This gives our model a much more realistic feel, capturing scenarios where environmental fluctuations definitely matter.

By bringing noise into the picture, we're also able to investigate how solitons (those stable wave packets) behave in situations that were previously off-limits using simpler, deterministic methods. Our findings tie in with recent progress in the field of nonlinear optics with noise, supporting the idea that, surprisingly, noise isn't always a negative influence—it can actually help keep solitons stable and coherent under specific conditions.

Future Work and Applications

Future work could aim to generalize these results to tackle more complicated cases that involve higher-dimensional objects, polarization-dependent noise, and other forms of nonlinearities such as saturation or log. It would also be extremely beneficial to experimentally demonstrate these soliton solutions in an experiment and assess their usefulness in photonic integrated circuits and quantum information processing systems.

In summary, there is a robust theoretical and numerical model for describing the behavior of optical solitons in real-world magneto-optical scenarios described in this work. It provides new ideas about how noise might be beneficial in allowing solitons to propagate and remain stable.

7. Conclusions

This study extends the understanding of optical solitone dynamics in analytically and numerically and numerically a disturbance-temporal spread, inter-model spread, dual-strength law nonlinearity, and a disturbance with multiplier white noise. Through the generalized Liénard equation and better direct algebraic method, we achieved diverse soliton solutions- including dark, bright, singular, straded and elliptical function types, which demonstrate their remarkable stability under noise disturbances. Severe, our findings suggest that the multiplier noise serves as a stable factor, which modifies its structural integrity and energy, modifying the soliton profile, challenging traditional assumptions about the disruptive role of noise. Including high-order dispersal effects provides a more realistic structure for modeling soliton proliferation in the practical environment. These results not only deepen theoretical insights, but also provide valuable guidelines for designing noisy-flexible optical communication systems. Future work should detect high-dimensional geometric and experimental beliefs to pursue bridge theory with applications in photonic technologies.

Declarations

Competing interests The authors declare no competing interests.

References

[1] J. Vega-Guzman, M. Z. Ullah, M. Asma, Q. Zhou and A. Biswas, Dispersive solitons in magneto-optic waveguides, Superlattices and Microstructures, DOI: 10.1016/j.spmi.2017.01.020.

[2] W. B. Rabie, H. M. Ahmed and W. Hamdy, Exploration of new optical solitons in magneto-optical waveguide with coupled system of nonlinear Biswas–Milovic equation via Kudryashov's law using extended F-expansion method. Mathematics, 11 (2023) 300.

[3] E. M.E. Zayed, K. A.E. Alurrfi, R. A. Alshbear, On application of the new mapping method to magneto-optic waveguides having Kudryashov's law of refractive index, Optik, 287 (2023) 171072.

[4] E. M. Zayed, M. E. Alngar and R. M. Shohib, Optical solitons in magneto-optic waveguides for perturbed NLSE with Kerr law nonlinearity and spatio-temporal dispersion having multiplicative noise via Itô calculus, Optik, 276 (2023) 170682.

[5] S. Arshed, A. Arif, Soliton solutions of higher-order nonlinear Schrödinger equation (NLSE) and nonlinear Kudryashov's equation, Optik 209 (2020)164588.

[6] E. M. Zayed, M. E. Alngar, A. Biswas, M. Asma, M. Ekici, A. K. Alzahrani and M. R. Belic, Solitons in magneto–optic waveguides with Kudryashov's law of refractive index, Chaos, Solitons and Fractals, 140 (2020) 110129.

[7] A. Biswas, A. H. Arnous, M. Ekici, A. Sonmezoglu, A. R. Seadawy, Q. Zhou, et al, Optical soliton perturbation in magneto-optic waveguides, J. Nonlinear Opt. Phys. Mater, 27 (2018) 1850005.

[8] E. M.E. Zayed, R. M.A. Shohib, M. E.M. Alngar, T. A. Nofal, K. A. Gepreel, Y. Yıldırım, Cubic–quartic optical solitons with Biswas–Milovic equation having dual-power law nonlinearity using two integration algorithms, Optik, 265 (2022) 169453.

[9] M. I. Asjad, N. Ullah, H. U. Rehman and M. Inc, Construction of optical solitons of magneto-optic waveguides with anti-cubic law nonlinearity, Optical and Quantum Electronics, 53 (2021) 646.

[10] A. Biswas, M. Ekici, A. Sonmezoglu, M. R. Belic, Highly dispersive optical solitons with Kerr law nonlinearity by F-expansion, Optik, 181 (2019) 1028-1038.

[11] N.A. Kudryashov, Highly dispersive solitary wave solutions of perturbed nonlinear Schrödinger equations, Appl. Math. Comput. 371 (2020) 124972.

[12] N.A. Kudryashov, Solitary wave solutions of hierarchy with non-local nonlinearity, Appl. Math. Lett. 103 (2020) 106155.

[13] E.M.E. Zayed, M. El-Horbaty, M.E.M. Alngar, M. El-Shater, Dispersive optical solitons for stochastic Fokas-Lenells equation with multiplicative white noise, Eng 3 (2022) 523-540.

[14] E.M.E. Zayed, R.M.A. Shohib, M.E.M. Alngar, Dispersive optical solitons in birefringent fibers for stochastic Schrödinger–Hirota equation with parabolic law nonlinearity and spatiotemporal dispersion having multiplicative white noise, Optik 278 (2023) 170736.

[15] E.M.E. Zayed, R.M.A. Shohib, M.E.M. Alngar, A. Biswas, Y. Yildirim, A. Dakova, H. M. Alshehri, M. R. Belic, Optical solitons with sasa-sastuma model having multiplicative noise via Itô calculus, Ukrainian J. Phys. Opt. 23 (2022) 9-14.

[16] E. M. E. Zayed, M. E. M. Alngar, R. M. A. Shohib, A. Biswas, Y. Yıldırım, H. Triki, S. P. Moshokoa, H. M. Alshehri, Optical solitons in birefringent fibers with Sasa-Satsuma equation having multiplicative noise with Itô calculus, J. Nonlinear Opt. Phys. Mater. 32 (2023) 2350006.

[17] S. Khan, Stochastic perturbation of optical solitons having generalized anti-cubic nonlinearity with bandpass lters and multi-photon absorption, Optik 200 (2020) 163405.

[18] E. M. Zayed, M. E. Alngar, A. Biswas, M. Asma, M. Ekici, A. K. Alzahrani and M. R. Belic, Solitons in magneto–optic waveguides with Kudryashov's law of refractive index, Chaos, Solitons and Fractals, 140 (2020) 110129.

[19] M. Eslami, M. Mirzazadeh, B.F. Vajargah, A. Biswas, Optical solitons for the resonant nonlinear Schrödinger's equation with time-dependent coefficients by the first integral method, Optik, 125 (2014) 3107-3116.

[20] E. M. E. Zayed, K. A. E. Alurrfi, On solving two higher-order nonlinear PDEs describing the propagation of optical pulses in optic fibers using the $(G'/G, 1/G)$-expansion method, Ricerche di Matematica, 64 (2015) 167-194.

[21] M. H. Saleh, A. A. Altwaty, Optical Solitons of The Extended Gerdjikov-Ivanov Equation In DWDM System By Extended Simplest Equation Method, Appl Math Inf Sci, 14 (5) (2020), pp. 1-7.

[22] A. A. Altwaty, M. H. Saleh, B. Dumitru, Soliton and wave solutions to the extended Gerdjikov-Ivanov equation in DWDM system with auxiliary equation method, Math Sci Lett, 9 (3) (2020), pp. 57-63.

[23] A. A. Altwaty, M. H. Saleh, R. K. M. Bader, Optical solitons with ractional temporal evolution in fiber bragg gratings with generalized anti-cubic nonlinearity by the fractional Riccati method, Results Phys, 22 (20) (2021), Article 103872

[24] M. H. Saleh, A. A. Altwaty, Solitons and other solutions to the extended Gerdjikov-Ivanov equation in DWDM system by the $\exp(-\phi(\zeta))$-expansion method, Ricerche di Matematica (2022), 1–14

[25] A. A. Altwaty, Optical solitons in fiber bragg gratings for the coupled form of the nonlinear(2+1)-dimensional Kundu-Mukherjee-Naskar equation via four powerful techniques, Results Phys, 44 (2023), Article 106205.

[26] E. M. E. Zayed, M. E. M. Alngar, R. M. A. Shohib, Dispersive optical solitons to stochastic resonant NLSE with both spatio-temporal and inter-modal dispersions having multiplicative white noise, Mathematics, 10 (2022), 3197.

[27] E. M. E. Zayed, R. M. A. Shohib, Solitons and other solutions to the resonant nonlinear Schödinger equation with both spatio temporal and inter-modal dispersions using different techniques. Optik 158 (2018) 970–984.

[28] Q. Zhou, C. Wei, H. Zhang, J. Lu, H. Yu, P. Yaq, Q. Zhu, Exact solutions to the resonant nonlinear Schödinger equation with both spatio-temporal and inter-modal dispersions. Proc. Rom. Acad. A 2016, 17, 307-313.

[29] A. H. Arnous, M. S. Hashemi, K. S. Nisar, M. Shakeel, J. Ahmad, I. Ahmad, R. Jan, A. Ali, M. Kapoor, N. A. Shah, Investigating solitary wave solutions with enhanced algebraic method for new extended Sakovich equations in fluid dynamics. Results in Physics, 57 (2024) 107369.

[30] X. L. Yang, J. S. Tang, Exact solutions to the generalized Liénard equation and its applications, Pramana 71 (2008) 1231-1245.

[31] K. A. E. Alurrfi, A. M. Shahoot, O. I. Elhasadi, Exact solutions for the GKdV–mKdV equation with higher-order nonlinear terms using the generalized $(G'/G, 1/G)$-expansion method and the generalized Liénard equation, Ricerche di Matematica, 73 (2024) 887-905.